Design and Experimental Study of a Miniature Ion Thruster

IEPC-2019-175

Presented at the 36th International Electric Propulsion Conference
University of Vienna • Vienna, Austria
September 15-20, 2019

Kun-Long Wu[1]
School of Astronautics, Beihang University, Beijing, 102206, China

Hao Huang[2]
Shanghai Institute of Space Propulsion, Shanghai, 201112, China

Jun-Xue Ren[3], Tian-Nan Yuan[4], Chao Lu[5], Yi-Ze Liu[6],
School of Astronautics, Beihang University, Beijing, 102206, China

Guang-Chuan Zhang[7], Hai-Bin Tang[8]
School of Space and Environment, Beihang University, Beijing, 102206, China

Abstract: Axial ring-cusp hybrid (ARCH) magnetic field may reduce electron loss on the anode to improve efficiency of the miniature in thruster by combining the axial and the ring-cusp magnetic field. Because of the change of magnetic field configuration, the traditional energy model of the discharge chamber is no longer suitable for the ARCH discharge. In this paper, based on the Goebel discharge performance model, a new discharge performance model for miniature ion thruster with the ARCH magnetic field is presented. Results of the model match well with the simulation results in reference. An ARCH miniature ion thruster with a small hollow cathode was designed and tested. The experimental results show that the maximum propellant utilization rate of the thruster reaches 60% and the thrust is 0.17-0.37mN at 300V screen grid voltage. The discharge losses are between 1800-6400watt/A, model analysis indicate that excessive emission current loss to the anode lead to high discharge losses.

Nomenclature

P_{exi}	=	total excited energy
n_o	=	neutral density
n_e	=	electron density
σ_*	=	excitation cross section
v_e	=	plasma electron velocity
V	=	plasma volume
ε^*	=	xenon excitation potential
n_p	=	primary electron density
v_p	=	primary electron velocity
D_B	=	diffusion coefficient perpendicular to the magnetic field of the plasma electron
k	=	Boltzman's constant

[1] Graduate Student, Joint Laboratory of Plasma & Propulsion, wklbuaa@163.com.
[2] Senior Engineer, Electric Propulsion Department, 775755494@qq.com.
[3] Associate Professor, Joint Laboratory of Plasma & Propulsion, rjx_buaa@163.com.
[4] Graduate Student, Joint Laboratory of Plasma & Propulsion, tiannany@buaa.edu.cn.
[5] Graduate Student, Joint Laboratory of Plasma & Propulsion, lc1142072767@126.com.
[6] Graduate Student, Joint Laboratory of Plasma & Propulsion, strutter112358@gmail.com.
[7] Doctor, Joint Laboratory of Plasma & Propulsion, zhanggchuan@126.com.
[8] Professor, Joint Laboratory of Plasma & Propulsion, thb@buaa.edu.cn.

T_e = electron temperature
e = electron charge
B = magnetic field strength
I_a = plasma electron current to the anode
∇n = electron density gradient
A_{as} = anode surface area
φ = plasma potential relative to anode
l_k = radial thickness of the edge magnetic field
A_i = total ion loss area
A_{ir} = ion loss area at the rear plate
A_{ia} = ion loss area at the anode
A_{is} = ion loss area at the screen grid
A_r = rear plate area exposed to plasma
f_{cr} = ion confinement factor of the magnetic field between ring-cusps
A_a = plasma electron loss and ion loss area at ring-cusp
f_{ca} = ion confinement factor of the edge magnetic field
A_S = grid area
T = effective grid transparency
I_i = ion loss current
I_{ele} = electron loss current
v_a = ion acoustic velocity
m = electron mass
I_L = primary current lost to anode
I_{ia} = ion current to the anode
I_s = ion current to the screen grid

I.Introduction

With the miniaturization of spacecraft, the need for low-power electric propulsion is put forward. Miniature ion thrusters are well suited for future space missions that require high efficiency, precision thrust, and low contamination in the mN to sub-mN range. [1] Conventionally sized ion thrusters, typically 25-30 cm in diameter are highly efficient. Miniaturization to the 3 cm scale requires careful consideration of the plasma structure and behavior of the ring-cusp discharge to maintain desirable performance.[2] For the standard ring-cusp configurations, the plasma structure is dominated by the cusp fields at the miniature scale and primary electron loss to the walls likely dominates discharge losses at this scale. [3]

Miniature Xenon Ion (MiXI) thruster， the early miniature ion xenon thruster ever designed is originally developed by Richard Wirz[4] at the California Institute of Technology. David W. Knapp[5] at California Polytechnic State University, in collaboration with Wirz, developed MiXI-CP-V3 with a ¼ inch hollow cathode and 3x3mm plasma confinement magnets in order to improve the plasma confinement characteristics, reliability, and performance of the MiXI design. However, miniature ring-cusp plasma behavior is dominated by the magnetic fields from the cusps, this can lead to high loss rates of high-energy primary electrons to the anode walls. The primary electron confinement was shown to considerably improve by imposing an axial magnetic field or by using cathode terminating cusps. [6,7] The ARCH magnetic field combines the characteristics of the axial magnetic field and the ring-cusp magnetic field. Two concentric axially magnetized magnetic forms an axial arched magnetic field and a constant current coil wound around the outer wall of the anode generates a stable induced magnetic field which is parallel to the inner wall of the anode. Compared with the ring-cusp magnetic field, the permanent magnet in the ARCH magnetic field is far from the plane of the optical system. Magnetic strength near the extraction plane is negligible and the radial gradient is small, therefore the beam current is extracted uniformly. At the same time, regulable coil current generates a medium-intensity edge magnetic field, thereby a reasonable anode current can be obtained while effectively confining electrons.

In this paper, based on the ARCH magnetic field and a small hollow cathode, a miniature ion thruster is designed and the performance experiment is carried out. The discharge performance model of the miniature ion thruster is studied.

II.Thruster design

Fig. 1 shows the initial structure of a miniature ion thruster with a 3cm discharge chamber diameter. Two concentric magnetic rings are installed upstream of the discharge chamber, which together with the magnetic coil wound around the anode produces an ARCH magnetic field. The hollow cathode inserts to the discharge chamber and xenon flow is fed to the discharge chamber through the hollow cathode. The aperture diameter of the screen grid and the acceleration grid is 0.7mm and 0.2mm, the screen grid and the acceleration grid have 1160 apertures, respectively.

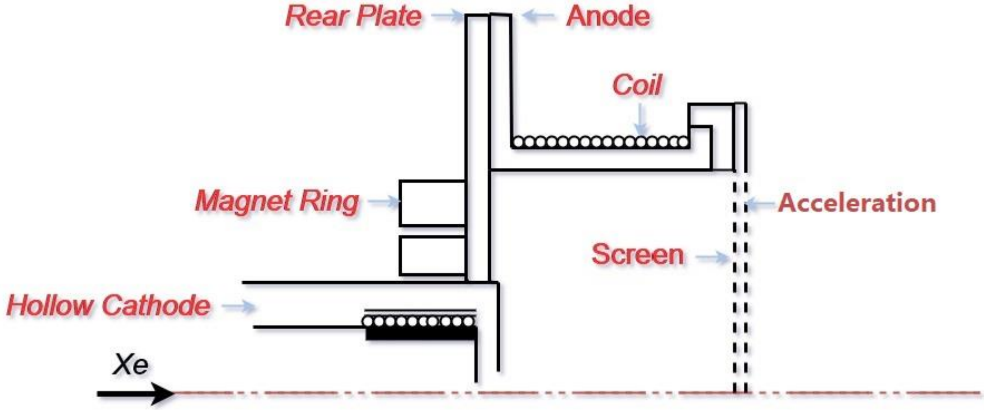

Figure 1. Diagram of the 3 cm diameter ARCH thruster with a hollow cathode, magnet ring, and coil.

A. Magnetic field simulation

Magnetic field is simulated with the magnetic module in COMSOL to design a magnetic field structure suitable for the small hollow cathode. The simulated magnetic field in Fig. 2 is composed of an arched magnetic field and an edge magnetic field parallels to the anode surface. Since the hollow cathode occupies the central portion of the upstream of the discharge chamber, the arched magnetic field presents a tilted form, but still constrains the primary electrons well. On the other hand, the edge magnetic field generated by the coil has a magnetic field strength of 50 Gs or more, the ion current loss to the anode is less than one-tenth of Bohm current, which is beneficial to increase the utilization rate of the propellant, thereby improving the thruster specific impulse. Downstream of the discharge chamber, the magnetic field strength near the screen and the radial magnetic field intensity gradient is negligible, which makes the plasma near the extraction plane more uniform, thereby increasing the uniformity of the extracted ion beam.

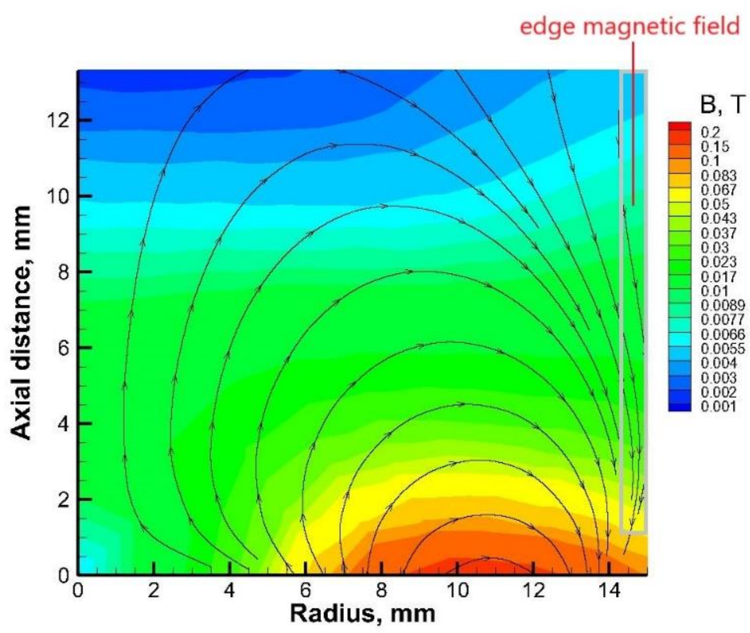

Figure 2. Simulation result of the ARCH magnetic field with 4A coil current.

Through the attempt of multiple magnetic field simulation, it is found that the samarium cobalt permanent magnet is a good choice to build the ARCH magnet. On the other hand, the simulation gives a series of design schemes for coil turns and coil current.

B. Thermal characteristic simulation

The main focus of the thermal characteristic simulation is the working temperature of the permanent magnet and the coil under the condition of adequate heated. The hot surfaces of the hollow cathode must be sufficiently downstream to avoid demagnetization of the cathode magnet at the back of the chamber. [1] Considering the cathode as an external homothermic heat source, the heat exchange between the plasma and surface of the discharge chamber can be divided into two aspects.

1. Thermal radiation between the plasma and surface of the discharge chamber.
2. The heat generated by the deposition of various charged particles on the surface of the discharge chamber.

The heat radiated by the plasma to the surface of the discharge chamber can be regarded as the deposition of its excitation energy on the chamber. The total radiant energy can be obtained by calculating the excitation energy:

$$P_{exi} = n_o n_e < \sigma_* v_e > V\varepsilon^* + n_o n_p < \sigma_* v_p > V\varepsilon^* \qquad (1)$$

According to the discharge performance model in Section Ⅲ, in the case of the maximum propellant flow rate and coil current of 4A, the particle energy deposition distribution of each surface of the discharge can be obtained as shown in Table. 1.

Table 1. Discharge chamber particle energy deposition

Current type	Current/A	Average energy loss /V	Energy/W
I_{ia}	0.031	12.8	0.40
I_L	0	32.8	0
I_a	0.941	21.8	20.5
I_s	0.047	52.8	2.48

Due to the existence of the edge magnetic field, the model considers that the primary electrons are difficult to directly impinge on the anode without collision. Therefore, the primary electron current lost to the anode can be neglected, and the current lost to the anode is dominated by plasma electrons. On the other hand, due to the limitation of the magnetic field, the ion current diffused to the anode is much smaller than the Bohm current.

According to the obtained energy calculation results, the thermal characteristics simulation was carried out by using COMSOL, it was observed that the system temperature became stable after about 100 s of operation, the temperature distribution as shown in Fig. 3 was obtained.

Fig. 3 reflects the temperature distribution of the thruster under the condition of adequate heated. The temperature of the coil and the magnet is concerned. According to the diagram, Samarium-cobalt magnets and high-temperature magnetic coils with a heat resistance of over 620 K are sufficient for the thruster.

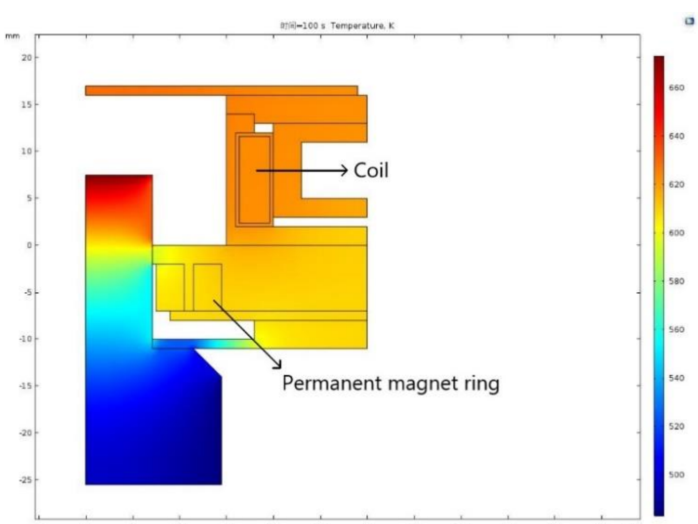

Figure 3. Discharge chamber thermal characteristics simulation results

C. Hollow Cathode

The hollow cathode uses barium tungsten emitter and the keeper diameter is 14mm. Performance test results show that the emission current is between 0.5-2A with the flow rate of 0.8-5sccm, the hollow cathode keeper voltage is 15-20V, and the keeper current is 1A.

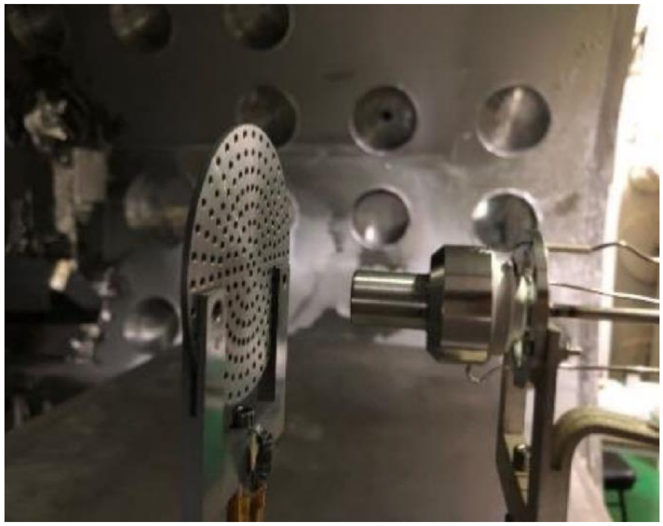

Figure 4. Hollow cathode experimental apparatus and the anode plate

III.Discharge performance model

The Goebel discharge performance model[8] was a current and energy balance zero-dimensional model of the plasma discharge in magnetic ring-cusp ion thrusters. The constraining effect of the ARCH magnetic field on the particles in the discharge chamber has a completely different performance between the edge magnetic field near the anode surface and the upstream ring-cusp magnetic field. Therefore, the traditional Goebel model cannot reflect the ARCH discharge performance well.

Upstream of the discharge chamber, the loss of primary electrons and secondary electrons are mainly concentrated at the ring-cusp. The loss of ions at the ring-cusp is often negligible, more ions cross the arch magnet between the ring-cusps and finally reach the rear plate. In this area, the traditional ring-cusp magnetic calculation method is applicable.

The edge magnetic field generated by the coil can be regarded as axial magnetic field. In the axial magnetic field, the primary electron is difficult to directly diffuse to the anode, and it is often necessary to generate conduction through the form of the collision to form a discharge loop, therefore, the loss of the primary electron can often be ignored. The diffusion of ions in the plasma to the anode is also affected by the magnetic field, if the magnetic field strength increases to about 50 Gs, the loss current of the anode reduces to 1/10 of the Bohm current.[9] For the axial magnetic field, the diffusion coefficient perpendicular to the magnetic field of the plasma electron is close to the Bohm diffusion coefficient, which can be expressed as Eq. 2[9].

$$D_B = \frac{1}{16}\frac{kT_e}{eB} \tag{2}$$

The electron current collected by the anode can be expressed as Eq. 3[9].

$$I_a = D_B e \nabla n A_{as} e^{\frac{e\varphi}{kT_e}} = \frac{1}{16}\frac{kT_e}{B}\nabla \mathrm{n}_e A_{as} e^{\frac{e\varphi}{kT_e}} \tag{3}$$

Combining the characteristics of the two magnetic fields, we give some new calculation formulas. The right side of Eq. (6) contain the electron loss in the magnetic cusp and the electron loss in the edge magnetic field.

$$A_i = A_{ir} + A_{ia} + A_{is} = A_r f_{cr} + A_a + A_{as} f_{ca} + A_S T \tag{4}$$

$$I_i = \frac{1}{2}(n_e + n_p) e v_a (A_r f_{cr} + A_{as} f_{ca} + A_a + A_S T) \tag{5}$$

$$I_{ele} = \frac{1}{4}\sqrt{\frac{8kT_e}{\pi m}} e n_e A_a e^{\frac{e\varphi}{kT_e}} + c\frac{1}{16}\frac{kT_e}{B}\frac{\mathrm{n}_e}{l_k} A_{as} e^{\frac{e\varphi}{kT_e}} \tag{6}$$

The Goebel model is complex, the complete form of the model can be referenced to Ref. [8]. The change of A_i, I_i, and I_a will affect the formula of the sheath potential, the discharge loss, and the like, which can be calculated by the Eq. (4)-(6) and Goebel model to build a new model suitable for the ARCH magnetic field. The discharge performance curve of ARCH V1 is obtained by the new model, which matches well with the Ref. [10] in Fig.5.

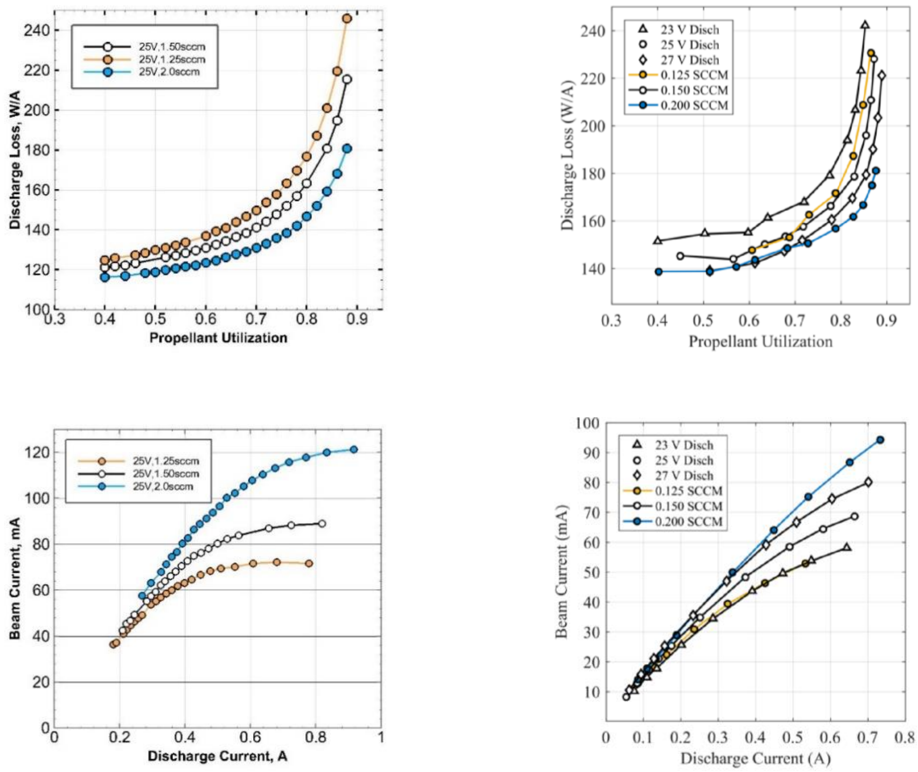

Figure 5. Left: ARCH V1 discharge performance curve and beam current vs. discharge current at a range of base neutral gas flow rates from the model. Right: ARCH V1 discharge performance curve and beam current vs. discharge current from Ref. [10].

In this work, the rear plate is made of the ceramic material, it is difficult to explain the effect between the ceramic surface and plasma. In this thesis, we think that the particle loss in ceramic surface can be ignored. Ion loss area at the rear plate, plasma electron loss and ion loss area at ring-cusp, and primary electron loss area at ring-cusp are taken as 0. According to our thruster structure and the discharge performance model, we obtain a discharge performance curve in different working conditions in Fig. 6 when the discharge voltage is 40V and the hollow keeper voltage is 20V.

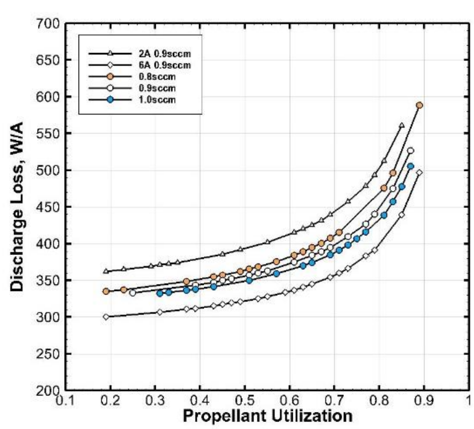

Figure 6. discharge performance of DT-IT4

IV. Experimental setup

Fig. 7 shows the circuit diagram of the experimental system, with separate power supplies for the ion thrusters, hollow cathodes, and magnetic coils. Due to the limitations of the experimental conditions, the thruster experiment used a single-grid structure. On the other hand, the lack of an acceleration grid results in the inability to use the neutralizer.

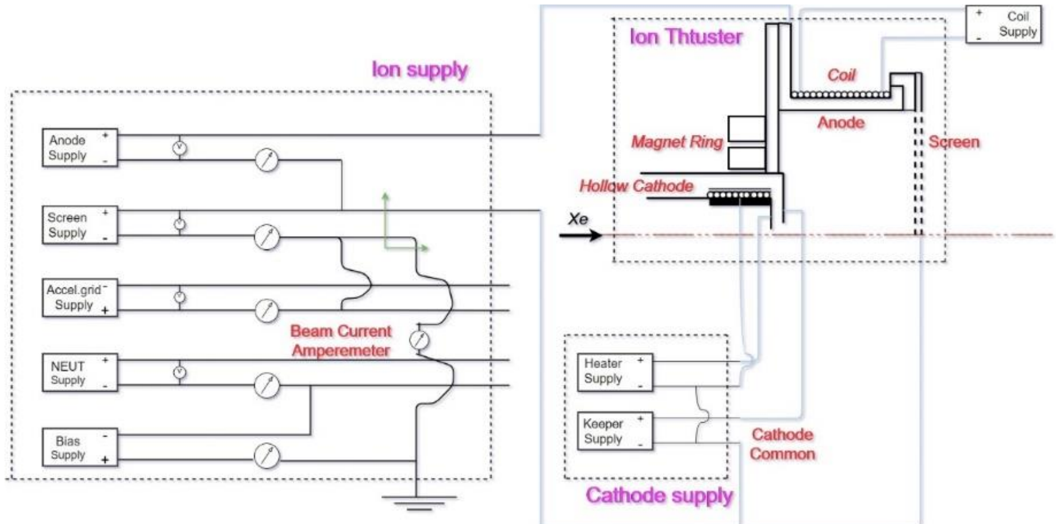

Figure 7. Diagram of the electrical system with the ion thruster, the cathode supply, the ion thruster supply, and the coil supply.

Fig. 8 shows the thrust-frame and ion thruster installation for the thrust measurement experiment. The experiment was carried out in a vacuum chamber with a vacuum of the $10^{-4}Pa$ level when the xenon feeds to the cathode at the flowrate of 0.8-1.4sccm. The thruster and the outboard equipment are connected through the wire and flange, the thrust stand is based on linearity between stress and strain of the pivot, equipped with a closed loop electromagnetic feedback. All wires and gas circuits connected to the static frame of the torsional-type thrust stand to ensure the accuracy of the thrust measurement result. The ignition experiment of ion thruster was carried out after the cathode ignition was successful. Due to the high cathode voltage drop, the anode voltage was adjusted to about 40V, then we can observe a distinct plume with a screen voltage of 300V.

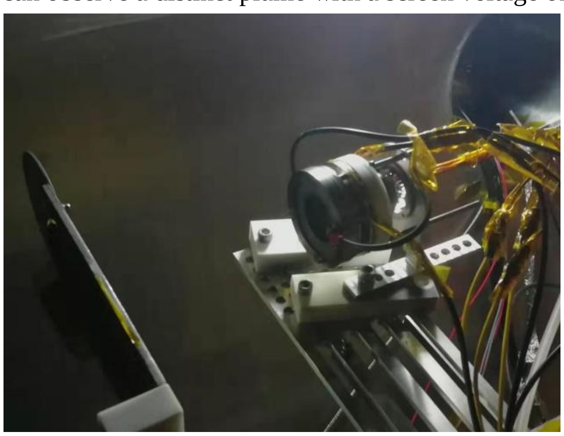
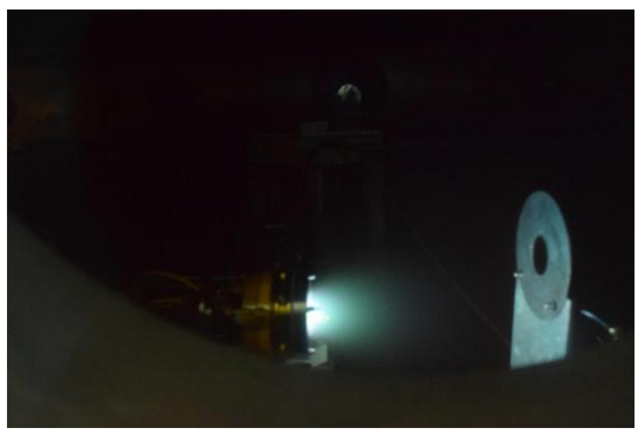

Figure 8. Left: ion thruster and thrust stand in the vacuum chamber. Right: plume of the thruster

V. Results and discussion

A. Thrust measurement result

In this work, the thrust and beam current of the thruster with a flow of 0.8sccm-1.4sccm were measured under the condition of the magnetic coil current of 2A, 4A, and 6A(as the coil current increases, the magnetic field strength of the edge magnetic field increases), under the condition that the screen voltage is 300V, the experimental results are obtained as shown in Fig. 9.

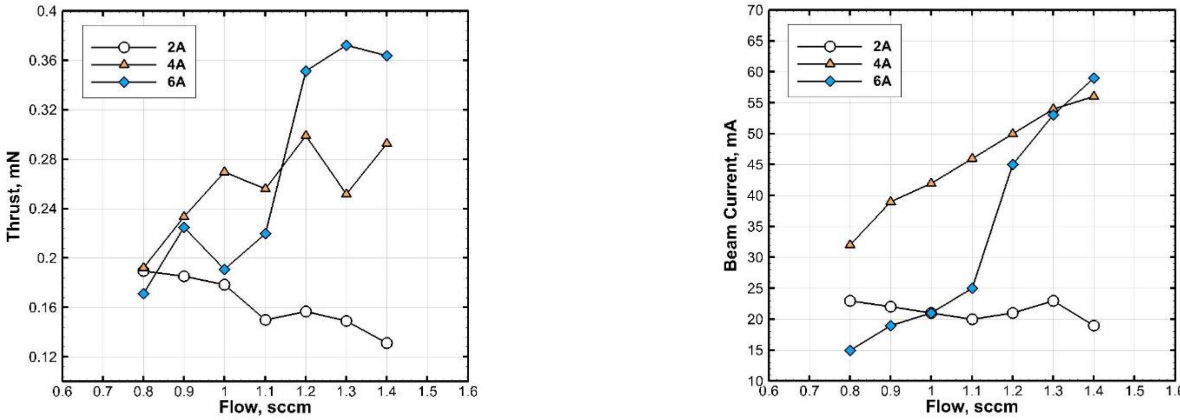

Figure 9. Thrust(left) and beam current(right) at a range of coil current and base neutral gas flow rates

According to Fig. 9, when the current of the coil is 2A, it is found that the thrust tends to slowly decrease with the increase of the flow rate. This phenomenon indicates that the magnetic field in the thruster is not strong enough to restrain the electrons in the case of the coil current of 2A. In the process of increasing the flow rate, the number of ions generated by ionization is not significantly improved, however, the number of atoms escaping from the screen grid is increasing, resulting in a collision of ions and atoms easily in beam current and ultimately leading to thrust loss.

In the case that the coil current is 4A, the magnetic field in the thruster has a moderate ability to constrain electrons. In the process of changing the flow rate from 0.8sccm to 1.0sccm, the atomic density is increasing, and simultaneously the ions generated by ionization increase significantly, which leads to the rise of thrust. But as the flow rate further increasing, the ion density increases slowly with the increase of the flow rate, therefore the increase of the thrust is suppressed due to the increase of the escaped atoms.

When the coil current is 6A, the magnetic field in the thruster has a strong ability to constrain electrons. As the flow rate increase, the ions generated by ionization in the discharge chamber increase continuously, the thrust tends to increase significantly. Based on the measuring result, in the case of large magnetic field strength, the magnetic field has a stronger ability to constrain electrons, a larger thrust is more easily obtained as the flow rate increases.

Fig. 9 shows the thrust and beam current at a range of flow and coil current. It can be found that the growth trends of thrust and beam current are roughly the same. This paper defines a new concept "effective thrust ratio", which represents the ratio of the measuring thrust and the thrust calculated by the measuring beam current. According to the experimental results, we obtain Fig. 10.

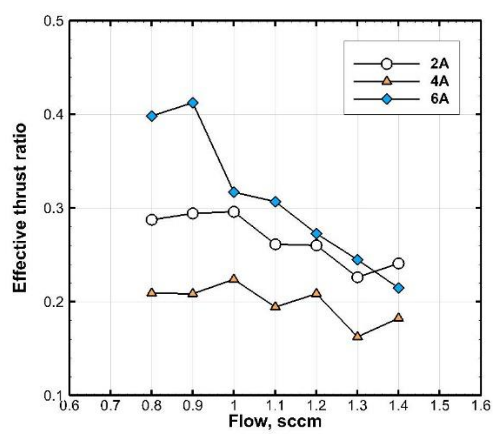

Figure 10. Effective thrust ratio at a range of coil current and base neutral gas flow rates.

The effective thrust ratio reflects the performance of the optical system. In this experiment, the thruster adopts a single-grid structure, which means a high atomic transmittance of the grid. A large number of neutral atoms are trapped in the beam current, resulting in a thrust loss. On the other hand, according to Fig. 9 and Fig. 10, we found that the effective thrust ratio of the thruster has a depressing tendency as the beam current increases. Fig. 11 answers this question, the beam divergence of the plume increases significantly with increasing beam current, which causes significant non-axial thrust loss. The reason for the non-axial loss is related to the absence of the acceleration grid and is also affected by the screen gate aperture. The screen grid aperture adopted in this work is 0.7mm, which is larger than a normal miniature ion thruster. A larger aperture means that the beam diameter increases and the space charge effect in the beam also increase so that the influence on the conductivity and the beam divergence angle is also increased. To obtain a better beam current performance, the size of the screen grid aperture should not be too large, it is feasible to increase the number of holes and decrease the aperture of the screen grid reasonably.

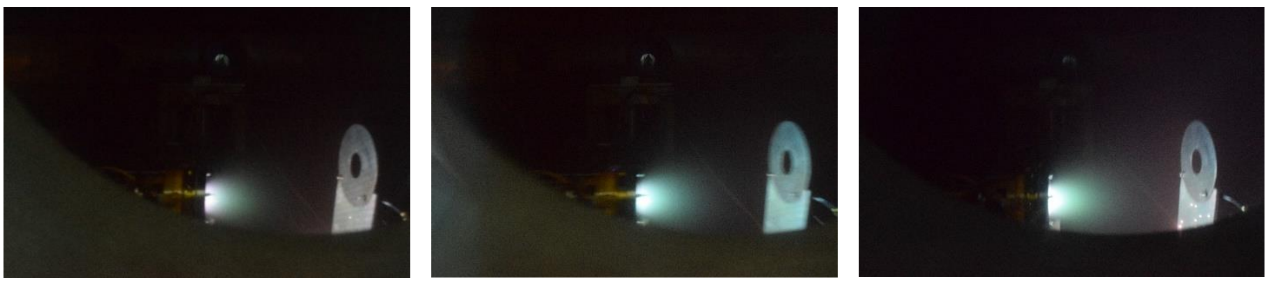

Figure 11. In the case of the same flow of 1.1sccm. Left: Thruster plume with a 20mA beam current. Middle: Thruster plume with a 25mA beam current. Right: Thruster plume with a 46mA beam current.

B. Propellant utilization

As shown in Fig. 12, When the coil current is 2A, the propellant utilization rate is generally low, and gradually decreases with the increase of the flow rate. This data shows that, in the case of low magnetic field strength, the degree of ionization in the discharge chamber is relatively low. The increase of flow not only fails to increase the ionization rate but also causes more propellant to be wasted. When the coil current is 4A, the propellant utilization rate is more than 50%, and it is barely influenced by the change of flow. Under the circumstances, the discharge room has a high ionization rate and the ions can be extracted well. When the coil current is 6A, the propellant utilization rate changes obviously with the increase of the flow rate. In the case of a low flow rate, the atomic density and the degree of ionization in the discharge chamber are not sufficiently high, but the magnetic constraint on the electron is large. This causes that xenon ions are extracted hardly for the quasi-neutrality of plasma. Although the maximum value for the plasma density is much higher in the strong magnet case, the field strength does not allow the plasma to spread throughout the chamber. Most importantly, it limits migration to the extraction region at the downstream end of the discharge. [11] In summary, the selection of the magnetic field strength of the ion thruster should match the propellant flow rate to achieve the best performance.

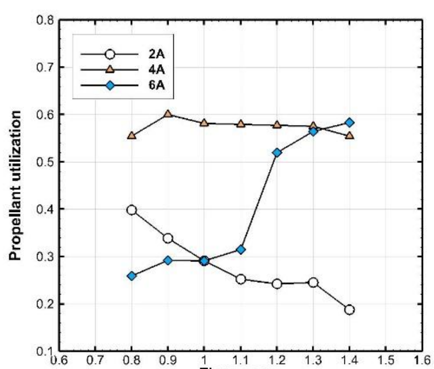

Figure 12. Propellant utilization at a range of coil current and base neutral gas flow rates.

C. Comparisons of model and experimental results

During the experimental measurement, it was found that the thruster discharge current was exorbitant. When the thruster was successfully ignited, the discharge current would increase rapidly from 0.2～1A to 2.4～3.2A, which caused the discharge loss of the thruster to increase greatly. Through the calculation of the experiment result, it is found that the hollow cathode has a large emission current. After a relatively stable discharge state is established in the discharge chamber, excessive emission current does not participate in the collision and heating reaction and directly reach the anode, lower primary electron utilization has a significant effect on discharge performance of miniature ion thruster. [9] Therefore, we have added these extra emission currents to the calculation of the simulate discharge loss to obtain a new thruster operating characteristic curve and compared with the actual measurement results.

Fig. 13 shows the comparison between the simulation results and the experimental results with the coil current of 2A. According to the experimental phenomenon and data and measurement, the emission current of about 2.4A is not involved in the ionization or heating reaction of the discharge. From the diagram, the model is in good contrast with the experimental results.

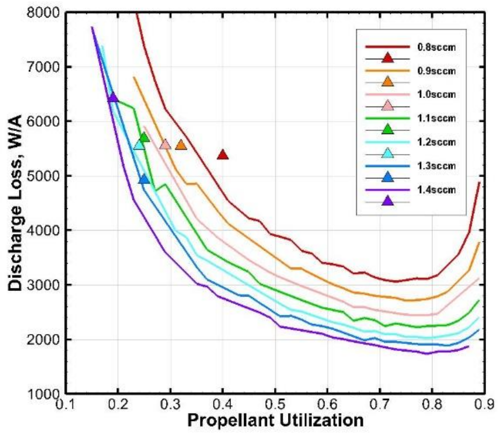

Figure 13. Model simulation and experimental results with coil current of 2A, the solid line is the working characteristic curve of the thruster calculated by the model and the point of the triangle is the experiment result.

Fig. 14 shows the simulation results of the model compared with the experimental results with the coil current of 4A and 6A. At this time, the magnetic field strength in the discharge chamber is relatively high, and the emission current directly lost in the discharge chamber is about 2A. From the diagram, there are some disparities between the calculation results of the model and the experimental measurements, but the trends are still approximate. Results of the model support the conjecture that the hollow cathode for our miniature ion thruster emits exorbitant electrons. A hollow cathode with the smaller emission current needs to be developed.

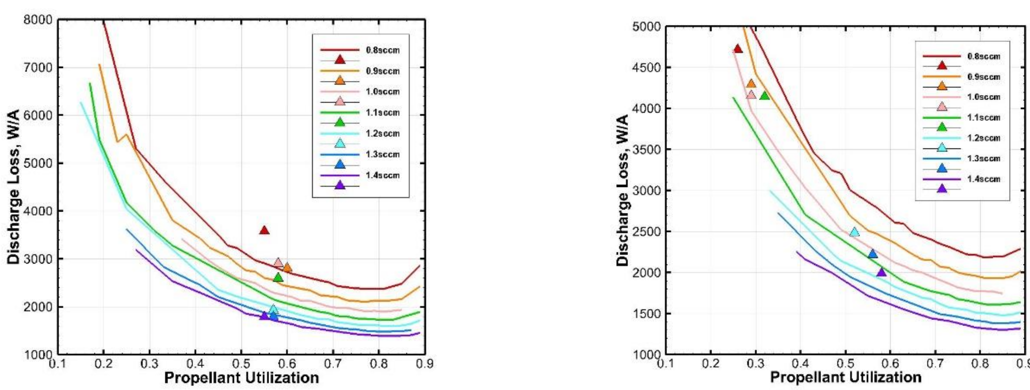

Figure 14. Left：Model simulation and experimental results with coil current of 4A. Right：Model simulation and experimental results with coil current of 6A.

VI.Conclusion

This work provides a case for the research of ARCH ion thruster with a hollow cathode. The zero-dimensional discharge performance model for the ARCH magnetic field is developed and proved to match well with the reference and experimental results. The model results verify that excessive emission current loss on the anode leads to high discharge losses. This assists the design of the ARCH thruster for better performance. The hollow cathode with smaller emission current is needed to get a better thruster efficiency. The next step will be to study the cathode with the smaller emission current and to the effect of material and structure of the rear plate on discharge performance.

Acknowledgments

This work was funded by the Innovation Foundation of Shanghai Institute of Space Propulsion. The authors acknowledge the support of the Beijing Vacuum Electronic Institution for the fabrication of the hollow cathode.

References

[1]Wirz, R., Sullivan, R., Przybylowski, J., Silva, M., "Discharge Hollow Cathode and Extraction Grid Analysis for the MiXI Ion Thruster," 42nd AIAA/ASME/SAE/ASEE Joint Propulsion Conference & Exhibit, Sacramento, California, USA, AIAA-2006-4498.

[2]Hann-Shin Mao, "Plasma Structure and Behavior of Miniature Ring-Cusp Discharges," Ph.D. Dissertation, Aerospace Engineering, University of California, Los Angeles, 2013.

[3]Dankongkakul, B., Wirz, R., "Design of Miniature Ring-Cusp Ion Thrusters via Analysis of Discharge EEDF and Plasma Parameter Mapping," *52nd AIAA/SAE/ASEE Joint Propulsion Conference*, Salt Lake City, UT, USA, AIAA-2016-4545.

[4]Wirz, R., "Discharge Plasma Processes of Ring-Cusp Ion Thrusters," Ph.D. Dissertation, California Institute of Technology, Pasadena, California, 2005.

[5]David W. K., "Implementation of a ¼ Inch Hollow Cathode into a Miniature Xenon Ion Thruster (MiXI)," Master Thesis, Science in Aerospace Engineering, California Polytechnic State University, San Luis Obispo, 2012.

[6]Dankongkakul, B., Wirz, R., "Design and Performance of the Axial Ring-Cusp Hybrid (ARCH) Discharge for Miniature Ion Thrusters," *35th International Electric Propulsion Conference*, Atlanta, Georgia, USA, IEPC-2017-295.

[7]Dankongkakul, B., Wirz, R., "Miniature ion thruster ring-cusp discharge performance and behavior," Journal of Applied Physics 122, 243303, 2017.

[8]Goebel, D. M., Wirz, R., Katz, I., "Analytical Ion Thruster Discharge Performance Model," Journal of Propulsion and Power, Vol. 23, No. 5, Sep-Oct. 2007.

[9]Goebel, D. M., Katz, I., *Fundamentals of Electric Propulsion: Ion and Hall Thrusters*, JPL Space Science and Technology Series, Jet Propulsion Laboratory California Institute of Technology, 2008.

[10]Dankongkakul, B., "Overcoming the Scaling Limitations of Ring-Cusp DC Ion Thruster Discharges," Ph.D. Dissertation, Aerospace Engineering, University of California, Los Angeles, 2017.

[11]Hann-Shin Mao, Wirz, R., "Plasma Structure of Miniature Ring-Cusp Ion Thruster Discharge," Journal of Propulsion and Power, Vol. 30, No. 3, May-June. 2014.